# The $^{31}P$ shielding in phosphine

Cynthia J. Jameson and Angel C. de Dios
*Department of Chemistry, M/C-111, University of Illinois at Chicago, P.O. Box 4348, Chicago, Illinois 60680*

A. Keith Jameson
*Department of Chemistry, Loyola University, Chicago, Illinois 60626*

(Received 26 July 1991; accepted 3 September 1991)

The temperature dependence of the phosphorus shielding in phosphine has been remeasured in the range 300–400 K in samples with densities in the range 7–30 amagat. The shielding surfaces are calculated using the localized orbital–local origin (LORG) method of Hansen and Bouman in terms of the symmetry coordinates for the molecule. These surfaces are used to calculate the rovibrationally averaged $^{31}P$ shielding. The calculated temperature dependence and the deuterium-induced isotope shift for phosphine are in agreement with experiment. The shapes of the $^{31}P$ in $PH_3$ and the $^{15}N$ in $NH_3$ shielding surfaces are very similar. With the exception of the inversion coordinate, the remarkable similarity of the surfaces becomes obvious when the shielding functions are scaled by the values of $\langle r^{-3} \rangle_{np}$ for the ground states of the neutral P and N atoms.

## INTRODUCTION

The observed value in the laboratory for the nuclear magnetic shielding is a consequence of an averaging over different nuclear configurations that the molecule can attain within the time period of the measurement. The measured shielding, like any molecular electronic property, results from an averaging that takes into account two surfaces, namely, the property and the potential. The property surface describes the behavior of the property upon changes in the nuclear arrangement while the potential surface governs the probability of finding the molecule at a given geometry. Measurements of the shielding at different temperatures or with involvement of various isotopomers can therefore provide an insight on how this property is altered by changes in the internal coordinates of the molecule in the vicinity of the equilibrium geometry. Conversely, the same theory of rovibrational averaging allows one to predict from a given shielding surface the isotope effects and the temperature dependence.

Deuterium-induced isotope shifts in several hydrides have long been reported and reviewed.[1–3] Without exception, the shielding of the atom bound to hydrogen is found to increase upon involving a heavier isotopomer. This apparently global characteristic has been noted before and explained by suggesting a universal negative first derivative of the shielding property with respect to bond extension.[4]

Shielding derivatives of both signs have been predicted theoretically.[5,6] Chesnut[5] finds that the shielding first derivative $(\partial\sigma/\partial r_{XH})_e$ in hydrides changes systematically in magnitude and sign across the periodic table. Positive first derivatives $(\partial\sigma/\partial r_{XH})_e$ were calculated in hydrides XH, where X is an electropositive element (LiH, BeH, $BH_3$, NaH, etc.), becoming negative for hydrides of electronegative elements. A reasonable explanation for this may be found in Ditchfield's observation that the direction of polarization of the electron distribution in a hydride dictates how the shielding behaves with bond extension.[6] However, because of the paucity of measurements of the isotope shifts induced in nuclei of the alkali or alkaline earth elements, the observed general trends in the large body of one-bond isotope shift data support a negative sign of the derivative.

To complement the isotope shift observations, there have been numerous gas-phase nuclear magnetic resonance (NMR) measurements at different temperatures done by Jameson and co-workers [references are cited in Refs. 7 and 8]. From this enormous amount of data on the temperature dependence of the $^{1}H$, $^{13}C$, $^{15}N$, $^{19}F$, $^{31}P$, $^{77}Se$, and $^{125}Te$ nuclear shielding in the gas phase in the limit of zero pressure, the generalization can be made that the nuclear magnetic shielding decreases with increasing temperature for most molecules. This observation is in agreement with the explanation given for the trends observed in isotope shifts. If the temperature dependence of the shielding is dominated by contributions from bond stretching, the shielding will decrease with increasing temperature due to an increase in the average bond length produced by rotation (centrifugal stretching) and by anharmonic vibration.

Amidst this comfortable agreement between the two experiments, a few exceptions have been found; the $^{31}P$ shielding in phosphine[9] and the $^{15}N$ shielding in ammonia.[10] Recently, a more precise measurement of the temperature dependence of the $^{15}N$ shielding in $NH_3$ has been made.[11] This was accompanied by *ab initio* calculations of the $^{15}N$ shielding surfaces in an attempt to reconcile the observed flat temperature dependence (which is exceptional) with the reported deuterium-induced isotope shift (which is of normal sign and magnitude). The two observations have been reconciled by the theoretical calculations. The inversion coordinate in $NH_3$ provides contributions to the shielding that have a temperature dependence in the opposite sense to that from all other displacement coordinates. Finally, the exceptional case of ammonia has found its proper place in the large congruent body of data that involve the temperature depen-

 0021-9606/91/249042-12$03.00 

dence of shielding and isotope shifts. It is hoped that the same will be achieved with the $^{31}P$ shielding in phosphine.

Samples of phosphine gas of densities in the range 7–30 amagat (1 amagat $= 2.687\times10^{19}$ molecules/cm$^3$) exhibit an exceptional temperature dependence for the $^{31}P$ shielding. The determination of the temperature dependence for the isolated molecule involves extrapolation of all data points to the zero density limit, which requires a precise evaluation of the temperature-dependent intermolecular effects. It has been observed that in samples where phosphine is present at low density ( $<1$ amagat) in mixtures with 10–30 amagat of argon, the temperature dependence of the $^{31}P$ shielding has already reversed into an opposite sense to what is observed in the higher-density pure $PH_3$ samples.[12] Clearly, if the temperature-dependent intermolecular effects are not properly accounted for, the remaining temperature dependence at the zero density limit may not reflect the isolated molecule's intrinsic temperature dependence. The earlier measurements had been made in a 2.1 T magnet.[9] In this present work, the $^{31}P$ resonance frequencies in samples at various densities are measured at 9.4 T. With a significant increase in sensitivity upon going to a higher field, a more accurate evaluation of the intermolecular effects is achieved.

An earlier work attempted to reconcile the deuterium-induced isotope shift with the exceptional temperature dependence for the $^{31}P$ shielding in phosphine.[13] However, a study of the rovibrational averaging of the internal coordinates of the molecule by itself can only provide limits for the phosphorus shielding changes upon extension of the P–H bond and upon distortion of the H–P–H bond angle. Without knowledge of the shielding surface, the interpretation of the observed temperature dependence and isotope effects on the $^{31}P$ shielding can not be complete. In this paper, systematic *ab initio* calculations of the phosphorus shielding surface for the phosphine molecule are reported. For the rovibrational averaging of the internal coordinates, the calculations will assume all vibrational amplitudes to be small and, unlike ammonia, limited to one minimum in the potential surface. The inversion barrier in phosphine is not as thermally accessible as that in ammonia.

The phosphorus shielding surface for the $PH_3$ molecule will be compared to that of the nitrogen shielding in ammonia in the hope of reaching a deeper understanding of the seemingly global observations for isotope shifts and the temperature dependence of the shielding. Any relationship discovered between these two cases and the two other molecules ($CH_4$ and $H_2O$) that have been previously studied may lead to some insight into the shielding surfaces for molecules not yet accessible to *ab initio* calculations.

## EXPERIMENT

$^{31}P$ spectra were obtained at 161.978 MHz in a Bruker AM-400 FT NMR spectrometer in sealed 4 mm (o.d.) tubes containing $PH_3$ at densities within the range 7–30 amagat. A typical spectrum had 500–2000 transients depending on the density of the sample. The digital resolution was, at least, 1 Hz per data point. The stability of the external magnetic field has been ascertained to 0.01 ppm by a method described elsewhere.[11] The resonance measurements were performed without proton decoupling in order to preserve the quartet, the presence of which aids in accurate phasing of the spectra.

The observed temperature dependence of the resonance frequency of $^{31}P$ in the various samples is displayed in Fig. 1. This is presented together with the other exceptional case of $^{15}N$ resonance frequency in $NH_3$. With these data points the intermolecular contribution on the shielding can be evaluated. The shielding dependence on density is expressed in a virial expansion.[14]

$$\sigma(T,\rho) = \sigma_0(T) + \sigma_1(T)\rho + \sigma_2(T)\rho^2 + \cdots. \quad (1)$$

Within the density range of this study, the dependence of the shielding on density is linear, hence, only the second virial coefficient can be obtained. From the $^{31}P$ data, we report

$$\sigma_1(T) \text{ ppb amagat}^{-1} = 77.8 - 0.250[T(K) - 300] + 2.26\times10^{-3}[T-300]^2 - 1.71\times10^{-5}[T-300]^3. \quad (2)$$

This temperature dependence of $\sigma_1$ is shown in Fig. 2. Again we present for comparison, the ammonia case. At each temperature, the value of $\sigma_1$ is determined from the slope of a linear plot of resonance frequency versus density. Due to the scatter in the data, the previous work did not have a well-defined temperature dependence for $\sigma_1$.[9] We can compare the results at 300 K. The new value, 77.8 ppb amagat$^{-1}$, is consistent with the previously reported value, 81.0

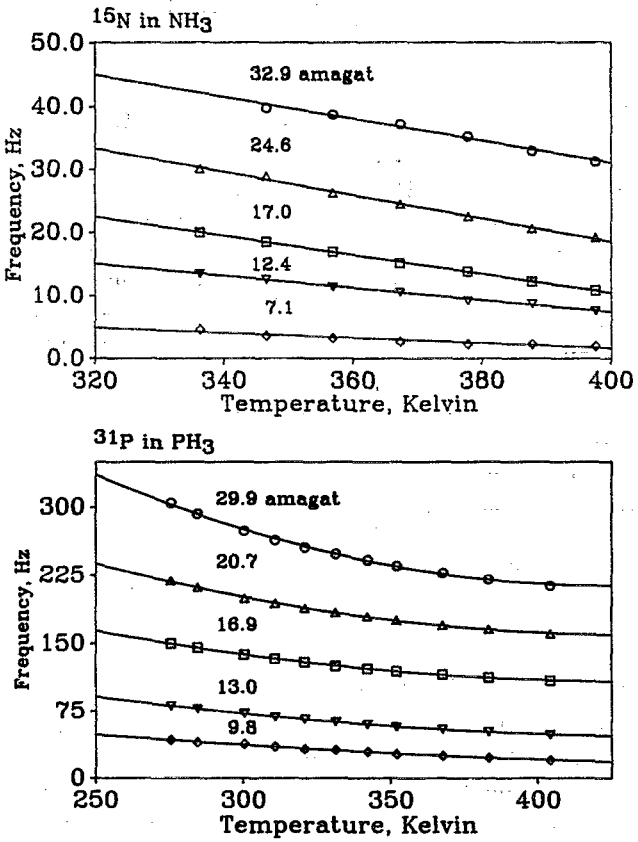


FIG. 1. (Top) Changes in the $^{15}N$ resonance frequencies at 40.56 MHz in $NH_3$ in the gas phase. (Bottom) Changes in the $^{31}P$ resonance frequencies at 161.98 MHz in $PH_3$ in the gas phase.

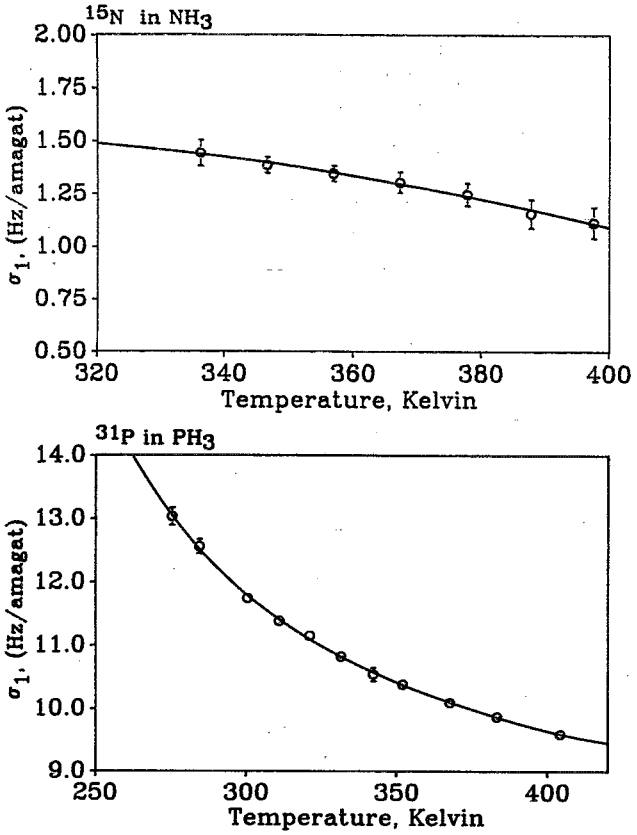


FIG. 2. The temperature dependence of the density coefficient of (top) the nitrogen chemical shift and (bottom) the phosphorus chemical shift.

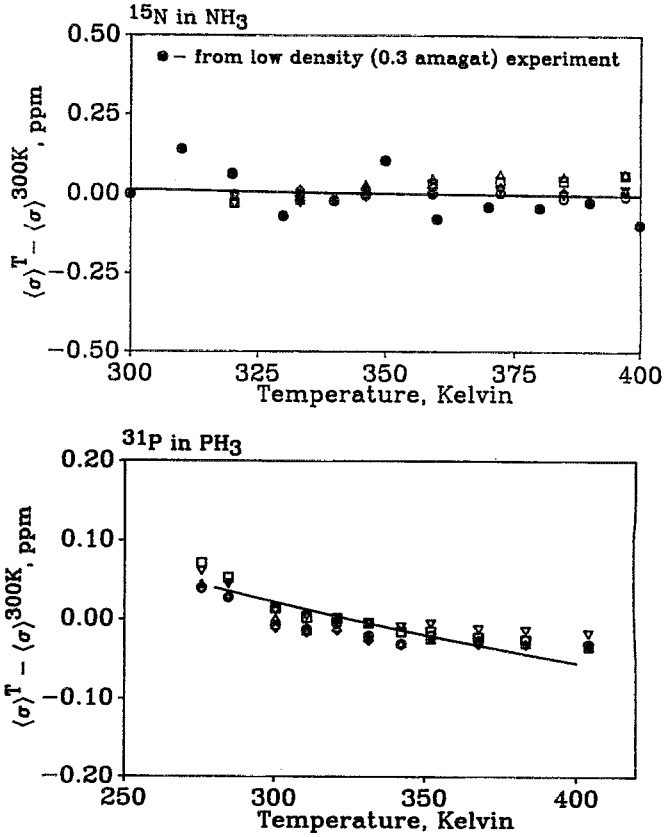


FIG. 3. (Top) The $^{15}$N shielding in the $NH_3$ molecule in the limit of zero density. (Bottom) The corresponding figure for the $^{31}$P shielding in the $PH_3$ molecule. The data points correspond to the data points from the individual samples shown in Fig. 1, using corresponding symbols. The lines are the computed temperature dependences from the *ab initio* theoretical calculations described herein.

ppb amagat$^{-1}$, after correction for bulk susceptibility.

Upon subtraction of $\sigma_1(T)\rho$ from each resonance frequency in Fig. 1, the $^{31}$P shielding in the isolated $PH_3$ molecule, $\sigma_0(T)$, is obtained at each temperature. Within experimental errors, this is consistent with the results obtained from very dilute mixtures of $PH_3$ in argon after subtraction of $\sigma_1(T)_{PH_3\text{–}Ar}\rho_{Ar}$.[12] The temperature dependence of the $^{31}$P shielding in the isolated $PH_3$ molecule is shown in Fig. 3 in comparison to that of the $^{15}$N shielding in $NH_3$. For $PH_3$, the deduced intrinsic temperature dependence of the isolated molecule is definitely in the opposite sense to the observed temperature dependence of the gas samples. The final result is that the $^{31}$P shielding in the isolated $PH_3$ molecule has a negative temperature coefficient, the same sign as for other nuclei in most molecules.

## COMPUTATIONAL DETAILS

It has been shown that conventional coupled Hartree–Fock calculations of nuclear shielding generally suffer from gauge origin difficulties even when large basis sets are used. This gauge problem has been solved in a practical way by using local gauge origins. There are several approaches which have been used for calculations of nuclear shielding: GIAO (gauge-including atomic orbitals) is a method introduced by Ditchfield[15] and recently modified and improved by Pulay *et al.*[16] IGLO (individual gauge for localized molecular orbitals) uses gauge factors associated not with individual atomic orbitals but with localized molecular orbitals. This approach by Schindler and Kutzelnigg[17] has been widely used. A third method LORG (localized orbital local origins) introduced by Hansen and Bouman,[18] avoids the computation of large terms of opposing sign by invoking identities and commutation relations to separate out those parts of the diamagnetic and paramagnetic terms that would have been identically equal and opposite in sign in the limit of a complete basis set. All the methods have the effect of damping of basis set errors in long range contributions to the shielding. All reference to the overall gauge origin is gone from the operating equations of the LORG and IGLO methods, and it has been shown that the operating equations are equivalent in the limit of a complete basis set.[19]

In this work the shielding calculations were performed with RPAC version 8.5 by Hansen and Bouman which employs the localized orbital local origin (LORG) method while GAUSSIAN88 provided the necessary SCF information.[20] The computations were carried out in an IBM 3090/300J/vector facility running CMS/SP under VM/XA.

The equilibrium geometry was chosen from experiment: $r_e = 1.4116$ Å and $\alpha_e = 93.33°$.[21] The standard 6-311G basis[22] augmented with one set of diffuse functions, three sets of $d$-polarization functions on phosphorus, and two sets of $p$-polarization functions on the hydrogens was used.

The phosphorus shielding in the phosphine molecule is calculated at different values of the following symmetry coordinates:

$$
\begin{aligned}
S_1 &= (1/\sqrt{3})(\Delta r_1 + \Delta r_2 + \Delta r_3), \\
S_2 &= (1/\sqrt{3}) r_e (\Delta\alpha_1 + \Delta\alpha_2 + \Delta\alpha_3), \\
S_{3a} &= (1/\sqrt{6})(2\Delta r_1 - \Delta r_2 - \Delta r_3), \\
S_{3b} &= (1/\sqrt{2})(\Delta r_2 - \Delta r_3), \\
S_{4a} &= (1/\sqrt{6}) r_e (2\Delta\alpha_1 - \Delta\alpha_2 - \Delta\alpha_3), \\
S_{4b} &= (1/\sqrt{2}) r_e (\Delta\alpha_2 - \Delta\alpha_3),
\end{aligned}
\tag{3}
$$

where $\Delta r$ and $\Delta\alpha$ refer to the deviation from the equilibrium bond length and bond angle, respectively. $S_1$ was varied from $-0.4$ to 0.4 Å encompassing 13 different geometries. For $S_2$, 12 points were used ranging from $-1.0$ to 1.0 Å. $S_3$ was changed up to 0.5 Å; this involved 11 points. Ten different configurations were considered for $S_4$; these points were within 1.0 Å from the equilibrium geometry. $S_3$ and $S_4$ are not totally symmetric; it is then assumed that the shielding is an even function of these coordinates. Sixteen additional geometries were considered for the extraction of the shielding mixed second derivative with respect to $S_1$ and $S_2$. Likewise, 16 more points were added in which $S_3$ and $S_4$ were varied simultaneously. All these points added to a total of 78 different geometries. The larger range for the coordinates involving bond angle distortions was chosen since these coordinates are related to motions which are of higher amplitude.

The rovibrational averaging of the shielding was done in the same fashion as in the treatment of $NH_3$,[11] with one major difference, the handling of the $S_2$ symmetry coordinate. The difference between the two molecules lies in their inversion potentials which are displayed in Fig. 4. The inversion potential function used for $NH_3$ in our previous work is the empirical one, obtained from Spirko, Stone, and Papousek.[23] For phosphine, the results from the SCF calculations done at different $S_2$ values provide the inversion potential. Using this potential function, numerical values of the inversion wave functions were obtained for phosphine. Comparing the two molecules, it is clear that the phosphine molecule is far more rigid than the ammonia molecule when it comes to the inversion motion. The numerical wave functions for phosphine are much more compact, localized at a pyramidal equilibirum geometry which is farther from the planar configuration than $NH_3$ was. As a result, the inversion motion is taken to be inaccessible in the $PH_3$ molecule at the temperatures of this study. The $S_2$ coordinate is therefore handled in exactly the same way as the other symmetry coordinates, that is, assuming small amplitude motions within the same energy minimum.

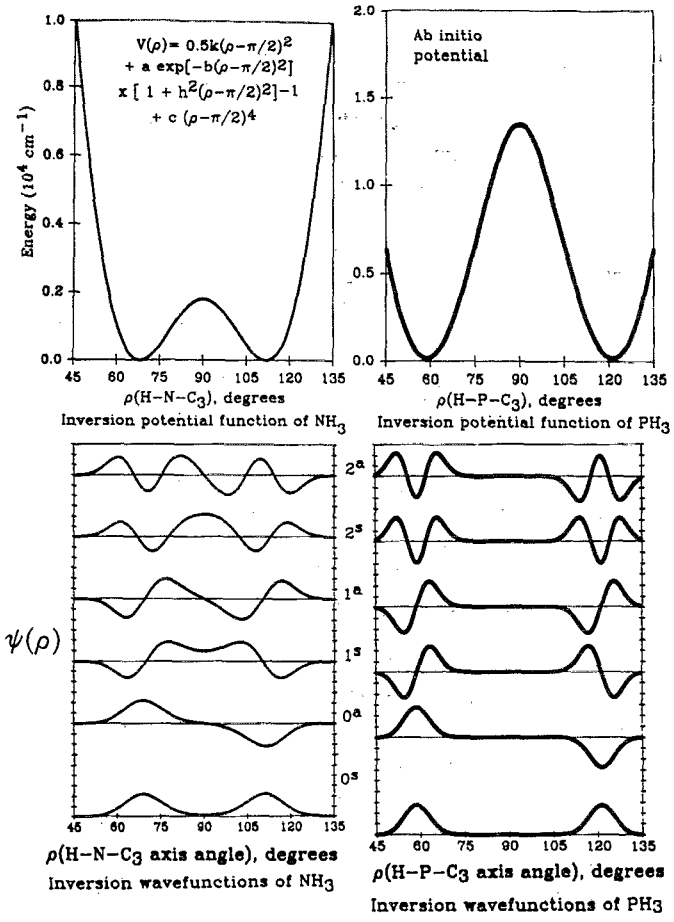


FIG. 4. A comparison of the two molecules, $NH_3$ and $PH_3$, with respect to the inversion mode is shown here.

The rovibrationally averaged value for the shielding at any temperature is obtained using the following equation:

$$
\begin{aligned}
P = {} & P_e + P_r(\Delta r_i;3) + P_\alpha(r_e)(\Delta\alpha_i;3) + \tfrac{1}{2}P_{rr}((\Delta r_i)^2;3) + P_{rs}(\Delta r_i \Delta r_j;3) \\
& + P_{r\alpha}(r_e)(\Delta r_i \Delta\alpha_i;3) + P_{r\beta}(r_e)(\Delta r_i \Delta\alpha_j;6) + \tfrac{1}{2}P_{\alpha\alpha}(r_e)^2((\Delta\alpha_i)^2;3) + P_{\alpha\beta}(r_e)^2(\Delta\alpha_i\Delta\alpha_j;3) \\
& + \text{higher order terms},
\end{aligned}
\tag{4}
$$

using the short-hand notation adopted by Raynes,[24] in which $(\Delta r_i; 3)$ stands for $(\Delta r_1 + \Delta r_2 + \Delta r_3)$. The derivatives of the shielding with respect to symmetry coordinates are obtained by fitting the numerical surface to power series in the coordinates. The derivatives of the shielding with respect to the internal coordinates were obtained from these using the relations given previously.[11] The thermal average values of the various internal coordinates at a given tempera-

ture were determined using Bartell's method[25] for the anharmonic contribution and the equation given by Toyama, Oka, and Morino for the centrifugal stretching contribution.[26] The force field for phosphine were taken from the work done by Duncan and McKean,[27] augmented by cubic force constants derived by including nonbonded interactions.

## RESULTS AND DISCUSSION

The results of the experiment for the temperature dependence of the $^{31}$P shielding in the isolated $PH_3$ molecule is definite: the temperature coefficient of the shielding is negative, i.e., the usual sign. As long as the temperature-dependent intermolecular effects are completely removed, the intrinsic temperature dependence of the $^{31}$P shielding in $PH_3$ molecule is no longer exceptional. The second virial coefficient in the expansion of the shielding in terms of density, $\sigma_1$, is unusually large for $^{31}$P in $PH_3$. This may be attributed to the small HPH bond angle that leaves the lone pair on the phosphorus atom more exposed to intermolecular interactions. It is also known that the $^{31}$P shielding in phosphine has a large gas-to-liquid shift, about 20 ppm.[12] For this reason, the $^{31}$P shielding difference between $PH_3$ and $PD_3$ has been remeasured in the gas phase and the value obtained is $2.5 \pm 0.1$ ppm (this work), fortunately in close agreement with the liquid phase data, $2.54 \pm 0.01$ ppm.[28] The intermolecular effects appear to be of comparable magnitude for both isotopomers and they nearly exactly cancel out in taking the difference. With this observation, it is probably safe to assume that the deuterium-induced isotope shift for the $^{15}$N shielding in $NH_3$ measured in the liquid phase by Wasylishen and co-workers[29] is not significantly different from its gas-phase value.

The *ab initio* calculations of the $^{31}$P shielding in $PH_3$ at the equilibrium geometry provide the parallel and perpendicular (to the $C_3$ symmetry axis of the molecule) components of the shielding tensor. Alternatively, we report the isotropic average shielding $\sigma_e \equiv (\sigma_\parallel + 2\sigma_\perp)/3$ and the shielding anisotropy $(\sigma_\parallel - \sigma_\perp)$. These are shown in Table I in comparison with other *ab initio* calculations. The conventional CHF results by Lazzereti and Zanasi[30] quoted in Table I are for the gauge origin at the phosphorus nucleus. The local origin methods, IGLO (independent gauge localized molecular orbitals) and the GIAO (gauge-including atomic orbitals) use molecular and atomic orbitals with gauge factors $\exp[(ie/2\hbar)(\mathbf{R}_k \times \mathbf{B})\cdot\mathbf{r}]$ in which $\mathbf{R}_k$ is the position vector of the centroid of charge of the localized molecular orbital or the atomic orbital, $\mathbf{B}$ the magnetic field, and $\mathbf{r}$ the position vector of the electron.[31,32] The SOLO (second-order local origin) calculations by Bouman and Hansen are LORG calculations that include second-order correlation effects.[33]

TABLE I. Comparison of results from various *ab initio* calculations of phosphorus shielding in phoshine.

| Method | Basis set | $\sigma_e$, ppm | $\sigma_\parallel - \sigma_\perp$, ppm | Ref. |
|---|---|---|---|---|
| This work[a] | 6-311 + G(3*d*,2*p*) | 597.33 | − 37.40 | |
| Conventional CHF | [10*s*6*p*3*d* /6*s*3*p*] | 577.56 | − 39.77 | 30 |
| IGLO[c] | [8*s*7*p*5*d* /3*s*2*p*] | 581 | − 29.4 | 31 |
| GIAO[d] | 6-1111 + G(3*d*) | 598.1 | − 32.8 | 32 |
| SOLO[e] | [6*s*4*p*2*d* /2*s*1*p*] | 594 | − 26.0 | 33 |

The molecular geometries used were as follows.
[a] $r_e = 1.4116$ Å, $\alpha_e = 93.3°$.
[b] $r_e = 1.417$ Å, $\alpha_e = 93.5°$.
[c] $r_e = 1.420$ Å, $\alpha_e = 93.3°$.
[d] $r_e = 1.42002$ Å, $\alpha_e = 93.3454°$.
[e] $r_e = 1.421$ Å, $\alpha_e = 93.3°$.

Agreement with the experimental isotropic value for shielding is satisfactory for $^{31}$P in $PH_3$ as for $^{15}$N in $NH_3$ (see Table II). The calculated value of the anisotropy for the $^{31}$P shielding in $PH_3$, however, is significantly lower than the experimental value. It is not clear what is needed to improve the calculations in $PH_3$ aside from increasing the size of the already relatively large basis set employed in this work; three sets of *d*-type polarization functions on the apex atom and two sets of *p*-type polarization functions on the hydrogen atoms. Hansen and Bouman have recently included correlation (second-order LORG or SOLO) in their calculation of the $^{31}$P shielding in $PH_3$;[33] the shielding anisotropy value they have obtained is even farther than ours from experiment (see Table I). The SOLO calculations used a basis set with two *d* functions (rather than 3) on phosphorus, and one *p* function (rather than 2) on hydrogen. We have found in this work that the differences in the results from calculations using three and two *d* functions are significant. However, the important conclusion in the SOLO calculations on $PH_3$ is that the second-order correlation contribution to the isotropic $^{31}$P shielding in the $PH_3$ molecule is $-4.0$ ppm. A more important factor in the comparisons in Table II is the choice of molecular geometry. We find in this work that the $^{31}$P shielding in the $PH_3$ molecule is rather sensitive to the P–H bond length and the HPH bond angle. Unfortunately, the various calculations in Table II were done at different molecular geometries, so that the results are not directly comparable. In particular, the SOLO results were obtained at $r_0 = 1.421$ Å rather than $r_e = 1.4116$ Å. Based on the now known shielding change with P–H bond length, the SOLO result for the isotropic shielding $\sigma_e$ could have been 4.83 ppm larger or 598.8 ppm.

It should also be noted that the experimental values at equilibrium geometry have been derived from the measured spin rotation tensors of $^{14}$N in $NH_3$ and $^{31}$P in $PH_3$ at the ground vibrational states and have not been corrected for zero-point vibration. Such corrections may well make the comparison of our theoretical isotropic $\sigma_e$ with experiment less ideal than appears to be the case in Table II.

The absolute shielding values, with which our calculations are to be compared, are derived from the spin rotation tensors measured in molecular beam electric resonance spectroscopy,[34] using the relations[35]

$$\sigma_\parallel = \left(\frac{m_p}{2m_e g_N}\right)\left(\frac{C^{zz}}{B^{zz}}\right) - \frac{e^2}{2m_e c^2}\sum_{N'} Z_{N'}\left(\frac{y^2+x^2}{R^3}\right)_{NN'} + \sigma_\parallel^d, \qquad (5)$$

TABLE II. Comparison with experiment.

| | $\sigma_e$ | | $\sigma_\parallel - \sigma_\perp$ | | $\sigma(XD_3) - \sigma(XH_3)$ | |
|---|---|---|---|---|---|---|
| | $NH_3$ | $PH_3$ | $NH_3$ | $PH_3$ | $NH_3$ | $PH_3$ |
| This work | 263.99 | 597.33 | − 38.00 | − 37.40 | 2.36 | 3.45 |
| Expt. | 264.5[a] | 594.45[b,e] | − 40[a] | − 55.98[b] | 1.87[c] | 2.54[d] |

[a] Reference 46.
[b] Reference 34.
[c] Reference 29.
[d] Reference 28.
[e] See text for improved values for $PH_3$: 599.93 and − 64.5 ppm.

$$\sigma_\perp = \left(\frac{m_p}{2m_e g_N}\right)\left(\frac{C^{xx}}{B^{xx}}\right) - \frac{e^2}{2m_e c^2}\sum_{N'} Z_{N'}\left(\frac{y^2+z^2}{R^3}\right)_{NN'} + \sigma_\perp^d, \quad (6)$$

where $C^{zz}$ and $B^{zz}$ are the spin rotation and the molecular rotational constants for the $zz$ inertial axis, $g_N$ is the $g$ value of the $^{31}$P nucleus, $Z_{N'}$ are the atomic numbers of the nuclei (other than $^{31}$P) in the molecule. The term containing the summation of internuclear coordinates removes the nuclear contribution to the spin rotation. In establishing the absolute shielding of $^{31}$P in $PH_3$,[12] the following values $\sigma_\parallel^d = 979.99$ ppm and $\sigma_\perp^d = 981.52$ ppm (Ref. 36) were used. These are in very good agreement with the values obtained by using Flygare's approximation.[37] Thus, we can use the latter in formulating $\sigma_\parallel^d$ and $\sigma_\perp^d$ as a function of nuclear coordinates. The values of $C^{zz} = -116.38 \pm 0.32$ kHz and $C^{xx} = -114.90 \pm 0.13$ kHz are those for the zero-point vibrational state of $PH_3$.[34]

Let us consider the magnitudes of the rovibrational corrections to $C^{zz}$ and $C^{xx}$. As for any other electronic property, we may write the expansion in Eq. (4),

$$C^{zz} = C_e^{zz} + C_r^{zz}(\Delta r_i;3) + C_\alpha^{zz} r_e(\Delta\alpha_i;3) + \cdots \quad (7)$$

and similarly for $C^{xx}$, where $C_e^{zz}$ is the value at the equilibrium geometry of a rigid $PH_3$ molecule, and $C_r^{zz}$, $C_\alpha^{zz}$, $C_r^{xx}$, $C_\alpha^{xx}$, etc., are the derivatives in this specific case, those that we have referred to generally as $P_r$, $P_\alpha$, etc. From the shielding calculations as a function of geometry, we are able to obtain instantaneous values of $C^{xx}$, $C^{zz}$, by using the values of the rotational constants $B^{xx}$, $B^{zz}$ and the values of the diamagnetic shielding tensor $\sigma^d$ at the instantaneous nuclear configurations. The traces along the $S_1$ and $S_2$ symmetry coordinates on the surfaces $C^{zz}$ and $C^{xx}$ are shown in Fig. 5. We calculated the first- and second-order zero-point vibrational corrections to $C^{zz}$ and $C^{xx}$. The symmetry coordinates $S_3$ and $S_4$ contribute at second order, but these roughly cancel out each other as they do for shielding, so we calculated only the first-and second-order terms in $S_1$ and $S_2$. This provides a good estimate of rovibrational corrections to the spin rotation tensor, short of doing the full rovibrational averaging.

$$\langle C^{zz}\rangle_0 \approx C_e^{zz} + C_1^{zz}\langle S_1\rangle_0 + C_{11}^{zz}\langle S_1^2\rangle_0 + C_2^{zz}\langle S_2\rangle_0 + C_{22}^{zz}\langle S_2^2\rangle_0 \quad (8)$$

and similarly for $C^{xx}$. Thus,

$$\langle C^{zz}\rangle_0 = -116.38 \pm 0.32 \ kH_z \approx C_e^{zz} + 1.30 \text{ kHz}, \quad (9)$$

$$\langle C^{xx}\rangle_0 = -114.90 \pm 0.13 \ kH_z \approx C_e^{xx} - 1.45 \text{ kHz}. \quad (10)$$

These values of the spin rotation tensor elements at the equilibrium geometry provide the "experimental" values of the absolute shielding tensor of $^{31}$P in the $PH_3$ molecule via Eqs. (5) and (6). Our "best experimental" values of $\sigma_e$ and $(\sigma_\parallel - \sigma_\perp)$ are

$$\sigma_e = 599.93 \text{ ppm}, \quad (\sigma_\parallel - \sigma_\perp)_e = -64.5 \text{ ppm}. \quad (11)$$

The values of the shielding for $^{31}$P in phosphine calculated at different values of the symmetry coordinates are pre-

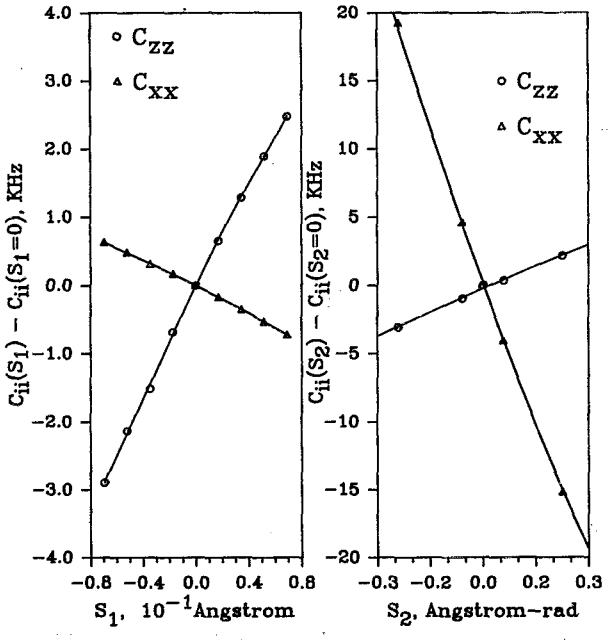


FIG. 5. The dependence of the spin rotation tensor components on the symmetry coordinates $S_1$ (left) and $S_2$ (right).

sented with the corresponding values of the $^{15}$N shielding in ammonia in Fig. 6 and 7. The shielding derivatives at the equilibrium geometry are

$P_1 = -257.78$ ppm/Å,
$P_2 = -151.99$ ppm/Å rad,
$P_{11} = -273.66$ ppm/Å$^2$,
$P_{22} = 189.622$ ppm/(Å rad)$^2$,
$P_{33} = -674.08$ ppm/Å$^2$,
$P_{44} = 78.562$ ppm/(Å rad)$^2$,
$P_{111} = -175.554$ ppm/Å$^3$,
$P_{222} = 196.614$ ppm/(Å rad)$^3$,
$P_{12} = -83.76$ ppm/Å$^2$ rad,
$P_{34} = -7.33$ ppm/Å$^2$ rad,
$P_{112} = -24.19$ ppm/Å$^3$ rad,
$P_{122} = -37.06$ ppm/Å$^3$ rad$^2$.

Except for the inversion coordinate, the shielding surfaces of $NH_3$ and $PH_3$ in Fig. 6 are remarkably similar. The similarity is made more obvious in Fig. 6 where the $^{31}$P shielding is arbitrarily scaled to $^{15}$N by a factor exactly equal to the ratio of $\langle 1/r^3 \rangle_{np}$ for the free P and N atoms in their ground state. The values $\langle 1/r^3 \rangle_{np}$ for the P and N atoms were obtained from the spin–orbit splittings in the spectra of the free atoms.[38]

The shielding as a function of the inversion coordinate is presented separately in Fig. 7 with the same scaling as in Fig. 6. For this symmetry coordinate, as might be expected, the shielding functions are qualitatively similar in shape. Both

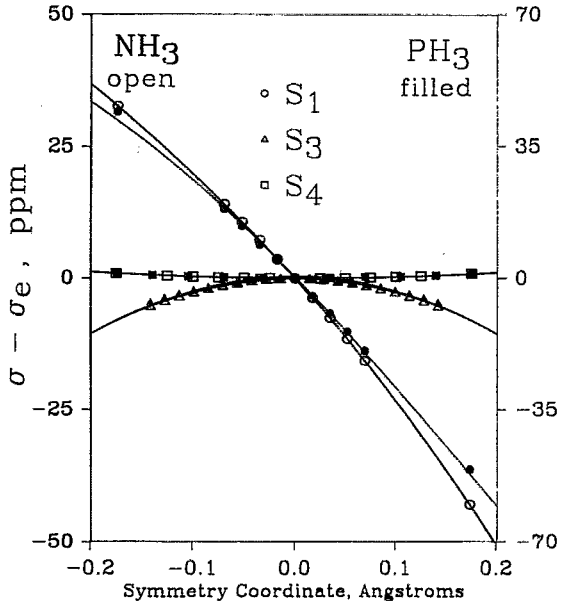


FIG. 6. The shielding functions for $^{31}$P in $PH_3$ and $^{15}$N in $NH_3$ as functions of the symmetry displacement coordinates. The vertical scales are related by the ratio of the values of $\langle r^{-3} \rangle_{np}$ for the ground states of the neutral P and N atoms.

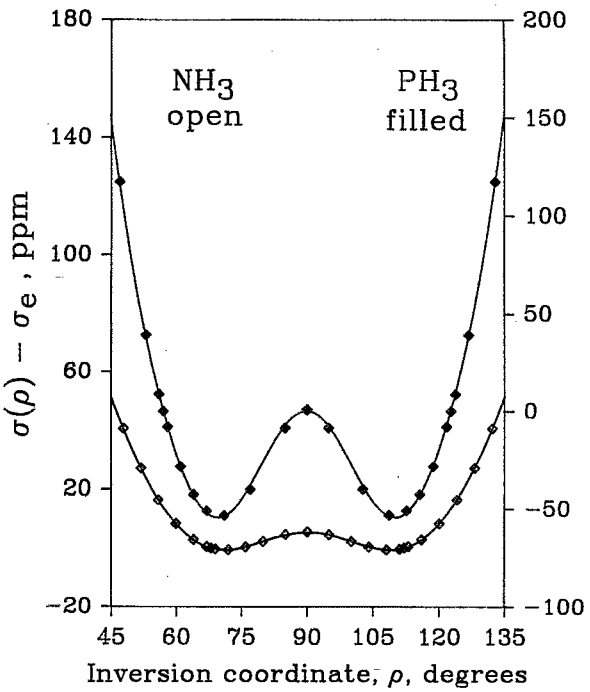


FIG. 7. The shielding for $^{31}$P in $PH_3$ and $^{15}$N in $NH_3$ as a function of the angle $\rho$ between the N–H (or P–H) bond and the $C_3$ symmetry axis of the molecule.

shielding surfaces have their minima occuring close to the tetrahedral angle. However, the surfaces cannot be superposed by arbitrary scaling because the two molecules differ in their bond angles at equilibrium geometry. For the shielding trace along the $S_2$ symmetry coordinate, a comparison can be made with the earlier work done by Chesnut and Foley.[32] Their results are very similar to ours in the short segment of the trace on the shielding surface between 80 and 120 deg for the HPH bond angle, the nonmonotonic behavior observed for the shielding across $S_2$ is attributed mainly to the perpendicular component of the shielding, $\sigma_\perp$. The component parallel to the symmetry axis simply decreases monotonically as the molecule shifts from pyramidal to planar geometry.

For the symmetry coordinates that are approximately superposable in $PH_3$ and $NH_3$, the scaling works remarkably well. Why so? The basis for the scaling of shielding values by the $\langle r^{-3} \rangle_{np}$ factors is the following:[39]

The energy term containing the nuclear shielding $\sigma^N$ is

$$E = \mu_N \cdot \sigma^N \cdot \mathbf{B} = -\frac{1}{c} \int \mathbf{A}_N \cdot \mathbf{j}(\mathbf{r}) d\tau, \tag{12}$$

where $\mathbf{A}_N$ is the magnetic vector potential due to the nuclear moment $\mu_N$ and can be chosen as

$$\mathbf{A}_N = (\mu_N \times \mathbf{r}_N)/r_N^3. \tag{13}$$

$\mathbf{r}_N$ is the position vector of the electron with respect to the nucleus $N$. The current density $\mathbf{j}(\mathbf{r})$ can be expanded in an order series:

$$\mathbf{j}(\mathbf{r}) = \mathbf{j}_0(\mathbf{r}) + \mathbf{j}_1^B(\mathbf{r}) + \mathbf{j}_2^B(\mathbf{r}) + \cdots, \tag{14}$$

where $\mathbf{j}_0(\mathbf{r})$ is the current density in the absence of the external magnetic field $\mathbf{B}$; $\mathbf{j}_1^B(\mathbf{r})$ is the current density contribution which is linear in the field, etc. The energy term in Eq. (12) is given by

$$\mu_N \cdot \frac{1}{c} \int (\mathbf{r}_N \times \mathbf{j}(\mathbf{r})) r_N^{-3} d\tau, \tag{15}$$

thus, the shielding field at nucleus $N$ does have an explicit $r_N^{-3}$ dependence. Both the paramagnetic and diamagnetic parts of the shielding are included here. These two parts are interconvertible via well-known identities, which have been used to advantage by Hansen and Bouman in formulating the LORG method.[18] Thus, the sensitivity of the nuclear magnetic shielding to changes in electronic structure or changes in molecular geometry depends on the extent to which the local magnetic field induced current densities are weighted by an inverse cube dependence on the distance from the nucleus in question. On the other hand, the electron density weighted by an inverse cube dependence on the distance from the nucleus in the free atom is experimentally available from the electron spin–electron orbit interaction constants for the free atoms and is found to have a periodic behavior with atomic number. Therefore, it is not entirely surprising that the changes in nuclear magnetic shielding of $^{31}$P in $PH_3$ and $^{15}$N in $NH_3$ with displacement coordinates of appropriate symmetry are nearly superposable when scaled according to the ratio of $\langle r^{-3} \rangle_{np}$ of the free phosphorus and nitrogen atoms. That the ranges of isotropic chemical shifts will scale as $\langle r^{-3} \rangle_{np}$ was predicted early in 1964,[40] long before multinuclear NMR data were widely available. This prediction has been found to hold remarkably well as the data have continued to accumulate. (For example, see Fig. 1 on p. 61 of Ref. 41.) The isotropic chemical shifts of nuclei in analogous compounds are found to scale by this factor; see, for example, the $^{77}$Se and $^{125}$Te case in Fig. 12.8 of Ref. 42. The scaling of the shielding surfaces for analogous molecules in the vicinity of their equilibrium geometries had been anticipated in the method of estimation of isotope shifts proposed in Ref. 43. More recently, the corresponding individual shielding tensor components in analogous compounds have been found by Zilm and co-workers to scale by this same factor.[44]

The derivatives of the shielding with respect to changes in the internal coordinates are presented in Table III. Our $P_r$ and $P_{rr}$ values, $-148.83$ ppm/Å and $-554.41$ ppm/Å$^2$, respectively, compare well with the derivatives; $-148.4$ ppm/Å and $-496.8$ ppm/Å$^2$ obtained by Chesnut using the GIAO method.[32] The thermal average values of the internal coordinates in $PH_3$ were calculated as described in Ref. 13, using the density of vibrational states in the harmonic approximation, which conveniently leads to

$$\langle v_i + \tfrac{1}{2} \rangle^T \approx \tfrac{1}{2} \coth(\hbar c \omega_i / 2kT). \tag{16}$$

Using these derivatives and the thermal average values of the internal coordinates in Eq. (4), the rovibrational corrections to the shielding can be obtained. Table IV shows that the rovibrational corrections which are second order in the stretch and bend are of comparable magnitude and of either sign. Although the second-order terms are not small, the second-order terms in the vibrational corrections to the $^{31}$P shielding nearly sum to zero as was found to be the case for $^{15}$N in $NH_3$. This is also true in the cases of $CH_4$ and $H_2O$.[45,24] Thus, the total vibrational correction to $^{31}$P shielding in the $PH_3$ molecule is nearly all (all but 1.4%) accounted for by the $P_r$ and $P_\alpha$ terms. By doing the calculations in the symmetry coordinates of the molecule, we avoid the arbitrary separation of bond stretch and bond angle contributions to shielding. We do find (see Table IV) that the mixed terms involving both bond extension and angle deformation coordinates constitute only a minor part of the entire rovibrational correction ($\leqslant 1\%$), and an even smaller fraction (less than 1 part per 1000) of the isotope shift. They do, however, constitute about 10% of the temperature dependence. We had found in the $NH_3$ molecule that the $P_{r\alpha}$ and $P_{r\beta}$ terms were less than 0.3% of the rovibrational correction in $NH_3$ or $ND_3$ and less than 0.15% of the isotope shift at 300 K, but contributed 6–17 % of the temperature dependence.

Unlike the case of $^{15}$N shielding in ammonia, the $^{31}$P shielding in phosphine as a function of $S_2$ does not have its minimum shielding close to the equilibrium geometry. As a result, the first-order contribution from bond angle distortions, $P_\alpha r_e \Delta\alpha$, is no longer insignificant. This is one major difference, but as mentioned previously, the two surfaces display a great deal of similarity with respect to the other symmetry coordinates. The first and second derivatives of the shielding function with respect to bond extensions are negative in both the $NH_3$ and $PH_3$ molecules. Rovibrational cor-

TABLE III. Shielding derivatives for $^{15}$N in $NH_3$ and $^{31}$P in $PH_3$.

| | $NH_3$ Ref. 11 | $PH_3$ This work |
|---|---|---|
| $P_r$ (ppm/Å) | −123.21 | −148.83 |
| $P_\alpha$ (ppm/Å rad) | −7.14 | −87.75 |
| $P_{rr}$ (ppm/Å$^2$) | −469.78 | −554.41 |
| $P_{\alpha\alpha}$ (ppm/Å$^2$ rad$^2$) | 79.11 | 115.58 |
| $P_{rs}$ (ppm/Å$^2$) | 244.81 | 371.97 |
| $P_{\alpha\beta}$ (ppm/Å$^2$ rad$^2$) | −3.98 | 10.83 |
| $P_{r\alpha}$ (ppm/Å$^2$ rad) | −6.47 | −32.81 |
| $P_{r\beta}$ (ppm/Å$^2$ rad) | −6.47 | −23.03 |

TABLE IV. Contributions (in ppm) of various terms in the $^{31}$P shielding in the $PH_3$ molecule.

| Term | Vibrational corr. at 300 K $\sigma(300\text{ K}) - \sigma_e$ $PH_3$ | $PD_3$ | Temp. dep. $\sigma(400\text{ K}) - \sigma(300\text{ K})$ $PH_3$ | $PD_3$ | Isotope shift $\sigma(PD_3) - \sigma(PH_3)$ 300 K | 400 K |
|---|---|---|---|---|---|---|
| $P_r$ | −9.16 | −6.72 | −0.175 | −0.229 | 2.440 | 2.386 |
| $P_{rr}$ | −5.97 | −4.29 | −0.002 | −0.015 | 1.678 | 1.665 |
| $P_\alpha$ | −3.29 | −2.54 | −0.070 | −0.159 | 0.744 | 0.655 |
| $P_{\alpha\alpha}$ | 5.54 | 4.13 | 0.173 | 0.311 | −1.411 | −1.262 |
| Mixed terms[a] | 0.10 | 0.10 | 0.008 | 0.010 | −0.002 | −1 E-4 |
| Total | −12.78 | −9.33 | −0.077 | −0.082 | 3.449 | 3.443 |

[a] $P_{rs} + P_{\alpha\beta} + P_{r\alpha} + P_{r\beta}$ terms.

rections coming from bond stretching are then expected to be negative, less so in the heavier isotopomers.

Table IV shows that the isotope shift is nearly entirely accounted for by the stretching contributions (terms in $P_r$ and $P_{rr}$). The rest, including the mixed terms, are opposite in sign and only about 2% in magnitude. The deuterium-induced isotope effect on the $^{31}P$ shielding in the phosphine molecule is the same sign (positive) as for $^{15}N$ shielding in ammonia because the isotope shift is dominated by bond stretching contributions in both cases.

In both $NH_3$ and $PH_3$, the calculated isotope shift is larger than what is observed in the laboratory. Since the isotope shift is dominated by stretching factors, the error lies in the calculation of the shielding at various symmetry coordinates that correspond to changes in bond length, that is, $S_1$ and $S_3$. The error present in the calculation of the shielding with respect to bond extension is primarily caused by the inability of the Hartree–Fock method in describing the molecule at large interatomic distances. The derivatives of the shielding with respect to $S_1$ and $S_3$ become overestimated. Calculations involving changes in the bond angle present difficulties, too. In fact, it has been shown that in ammonia the trace of the $^{15}N$ shielding function along the inversion coordinate is extremely sensitive to the choice of basis set.[13]

Based on our calculations, bond stretching contributions clearly dictate the deuterium-induced isotope shift in both $^{15}N$ in ammonia and $^{31}P$ in phosphine. If the measured isotope shifts are divided by $\langle r^{-3}\rangle_{np}$ of their corresponding apex atom, the results are 0.959 ppm for ammonia and 0.991 ppm for phosphine. This remarkable coincidence can be explained by the following conditions. First, the two molecules have comparable rovibrational corrections to the internal coordinate of bond stretching, $\Delta r$. Second, it has already been shown that the shielding functions of $S_1$ and $S_3$ scale accordingly. Last, the isotope shift is dominated by contributions from these coordinates. A scaling of the isotope shifts is thus possible. When these three conditions are met, one can expect a linear plot for the deuterium-induced isotope shift versus $\langle r^{-3}\rangle_{np}$ of the atom bound to hydrogen in Group VA hydrides. Unfortunately, there is little possibility of testing this because of the broad $^{75}As$ or $^{121}Sb$ NMR signals in $AsH_3$ and $SbH_3$ samples due to the efficient quadrupolar relaxation mechanism.

The temperature dependence, on the other hand, is less simply described. As in $NH_3$, the temperature dependence of the $^{31}P$ shielding in $PH_3$ comes from centrifugal stretching and, in addition and equally important, bond angle distortions. For $NH_3$, the two are opposing, leading to a very flat temperature dependence. $PH_3$ differs from $NH_3$ in this respect. Due to a significantly larger and negative $P_\alpha$, the first-order contribution resulting from symmetric bending and centrifugal distortion of the bond angles adds to the bond stretching contributions. Only the second-order contribution coming from the $P_{\alpha\alpha}$ term is of positive sign. Consequently, this results in a fairly well-defined negative temperature dependence for the $^{31}P$ shielding in $PH_3$ unlike the $^{15}N$ shielding in $NH_3$. For the intrinsic temperature dependence in these types of molecules, one can say that there is no single dominant contribution; its evaluation requires considering contributions from all symmetry coordinates. The temperature dependence due to changes in bond length comes mainly from centrifugal stretching. Its magnitude is primarily a result of large derivatives of the shielding with respect to stretching coordinates. On the other hand, although shielding derivatives of bond angle distortions are small, their significant contributions to the temperature dependence owe their magnitude to the greater amplitudes of the bending motions. In the case of ammonia and phosphine, it has been shown that the dependence of the nuclear shielding on one of the symmetry coordinates that involve changes in bond angles, $S_2$, is not straightforward. The temperature dependence considers a wider picture than the isotope shift does, hence, does not lend itself easily to a simple scaling procedure.

From centrifugal stretching alone, a negative temperature dependence is expected due to the negative shielding derivatives with respect to bond extension. In $NH_3$, it has been found that there are opposing contributions to the average shielding coming from the inversion coordinate. These contributions to the deuterium-induced $^{15}N$ isotope shift are small. On the other hand, they are significant enough to completely offset the negative temperature dependence due to bond stretching, leading to a very small overall temperature dependence for $^{15}N$ in $NH_3$ molecule. In the case of $PH_3$, the only opposing factors found are the second-order contributions from the $S_2$ and $S_4$ coordinates. The first-order contribution from bond angle distortion is also negative, reinforcing the contributions from bond stretching. It is consequently unequivocal that, in theory, the $^{31}P$ shielding in $PH_3$ should have a negative temperature dependence.

The *ab initio* calculated temperature dependence of the $^{15}N$ shielding in $NH_3$ and $^{31}P$ shielding in $PH_3$ are shown as curves for comparison with the experimental data points in Fig. 3. The experimental and theoretical results for the temperature coefficient of $^{31}P$ shielding in the $PH_3$ molecule are sufficiently large that a negative temperature dependence, which is normal, can be reported with confidence. A larger basis set may be employed in the hope of improving the calculations. However, the objectives of this work have already been achieved. Experimentally and theoretically, the $^{31}P$ shielding in $PH_3$ has been shown to have indubitably a negative temperature dependence which is in agreement with its reported deuterium-induced isotope shift and compatible with the large body of data observed for the nuclear shielding in other molecules.

With this work included, detailed calculations of shielding surfaces are now available for the heavy atom in the $H_2O$,[24] $CH_4$,[45] $NH_3$,[11] and $PH_3$ molecules. Let us examine these surfaces for general trends. For this purpose, Fig. 8 displays the traces on the shielding surfaces for $^{13}C$ in $CH_4$ and $^{17}O$ in $H_2O$ along the symmetry coordinates given in Table V. These are to be compared with Fig. 6 for $NH_3$ and $PH_3$. Not surprisingly, the traces along the $S_1$ symmetry coordinates, the totally symmetric stretch, all show that the shielding of the heavy nucleus decreases with bond extension. The traces are very similar; both the first and second derivatives are negative in each of the four molecules studied, and the change in shielding is most pronounced

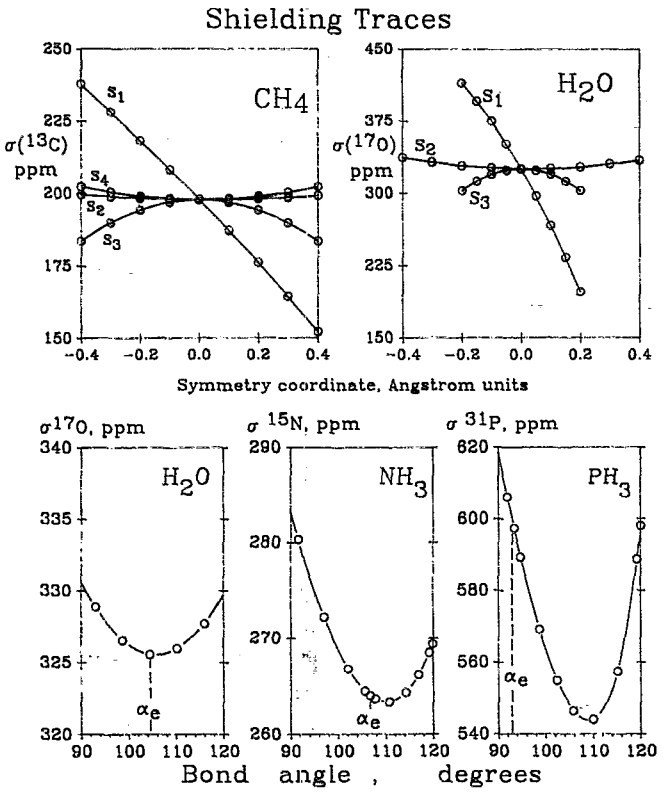


FIG. 8. (Top) Shielding traces for $^{13}C$ in $CH_4$ and $^{17}O$ in $H_2O$, to be compared with Fig. 6. (Bottom) The shielding as a function of the bond angle in $H_2O$, $NH_3$, and $PH_3$.

along the $S_1$ coordinate. The shape is also very similar to that calculated for diatomic molecules such as HF.[6] It is therefore not too surprising that one-bond isotope shifts, which are largely determined by $S_1$, appear to have global characteristics that mimic those in diatomic molecules.[7]

The shielding change along the asymmetric stretch coordinate $S_3$ appears to be similar in the four molecules. In each case the shielding surface is concave downward, i.e., displacements from the equilibrium geometry along this coordinate cause the shielding of the central atom to decrease; the second derivative $(\partial^2\sigma/\partial S_3^2)_e$ is negative and fairly large. On the other hand, the traces along the asymmetric bending ($S_4$) coordinate are concave upward in each case. The change in shielding with the asymmetric bend ($S_4$) is not as pronounced as the change in shielding with asymmetric stretch ($S_3$), i.e., $|(\partial^2\sigma/\partial S_4^2)|$ is less than $|(\partial^2\sigma/\partial S_3^2)|$. Nevertheless, these two largely cancel each other's contributions to the rovibrational effects for each molecule since vibrational frequencies for bends are generally lower than those for stretches. In methane, $S_2(E)$ helps $S_4(T_2)$ to offset the rovibrational effects of $S_3(T_2)$.

Finally, the change in shielding due to the totally symmetric bond angle deformations in the bent and pyramidal molecules are compared in the bottom half of Fig. 8. The shielding surfaces for $H_2O$, $NH_3$, and $PH_3$ are plotted here as functions of the bond angle, instead of the totally symmetric displacement coordinate $S_2$, in order to bring out the similarities. The most significant result is that all shielding surfaces have the minimum shielding at the tetrahedral angle. This was somewhat of a surprise. Whereas the fact that the planar configuration in $NH_3$ and $PH_3$ should correspond to an extremum in shielding is only to be expected by symmetry, it is not at all clear that the nuclear configuration corresponding to a tetrahedral bond angle should also be an extremum in the shielding surface. At the same time it appears unlikely that this is merely a coincidence. This remains a question to be answered. In each case, the increase in shielding towards angles smaller than tetrahedral is somewhat more pronounced than the increase with increasing bond angle towards angles larger than tetrahedral. The contributions of symmetric bond angle deformation to the rovibrational effects of shielding depend on the bond angle at the equilibrium molecular geometry, 104.5°, 106.7°, and 93.3° for $H_2O$, $NH_3$, and $PH_3$, respectively. The following comments have been made for the $H_2O$ case,[24] which fortuitously has a nearly tetrahedral equilibrium angle. "That $\sigma(O)$ reach minima at an angle coincidental with the energy can be tentatively rationalized by the argument that angle changes in either direction from equilibrium weaken the bonding so that $\sigma(O)$ approaches its atomic value which is larger than that for equilibrium." These cannot hold in general, as we now see, and are perhaps not applicable even to the $H_2O$ case.

TABLE V. Symmetry coordinates for Fig. 8.

| Symmetry coordinate | $H_2O$ | $NH_3$ or $PH_3$ | $CH_4$ |
|---|---|---|---|
| $S_1$ | $\frac{1}{2}[\Delta r_1 + \Delta r_2]$ | $3^{-1/2}[\Delta r_1 + \Delta r_2 + \Delta r_3]$ | $\frac{1}{2}[\Delta r_1 + \Delta r_2 + \Delta r_3 + \Delta r_4]$ |
| $S_2$ | $\Delta\alpha$ | $3^{-1/2}r_e[\Delta\alpha_1 + \Delta\alpha_2 + \Delta\alpha_3]$ | $(12)^{-1/2}r_e\begin{bmatrix} 2\Delta\alpha_1 - \Delta\alpha_2 \\ -\Delta\alpha_3 - \Delta\alpha_4 \\ -\Delta\alpha_5 + 2\Delta\alpha_6 \end{bmatrix}$[a] |
| $S_3$ | $\frac{1}{2}[\Delta r_1 - \Delta r_2]$ | $6^{-1/2}[2\Delta r_1 - \Delta r_2 - \Delta r_3]$[a] | $(12)^{-1/2}\begin{bmatrix} \Delta r_1 + \Delta r_2 + \Delta r_3 \\ -3\Delta r_4 \end{bmatrix}$[a] |
| $S_4$ | NONE | $6^{-1/2}r_e[2\Delta r_1 - \Delta r_2 - \Delta r_3]$[a] | $(12)^{-1/2}r_e\begin{bmatrix} 2\Delta\alpha_1 - \Delta\alpha_2 \\ -\Delta\alpha_3 - \Delta\alpha_4 \\ +\Delta\alpha_5 - 2\Delta\alpha_6 \end{bmatrix}$[a] |

[a] Only one representative of the symmetry coordinate is shown. $S_3$ is doubly degenerate in $NH_3$ and $PH_3$; $S_2$ is doubly degenerate in $CH_4$; $S_3$ and $S_4$ are triply degenerate in $CH_4$.

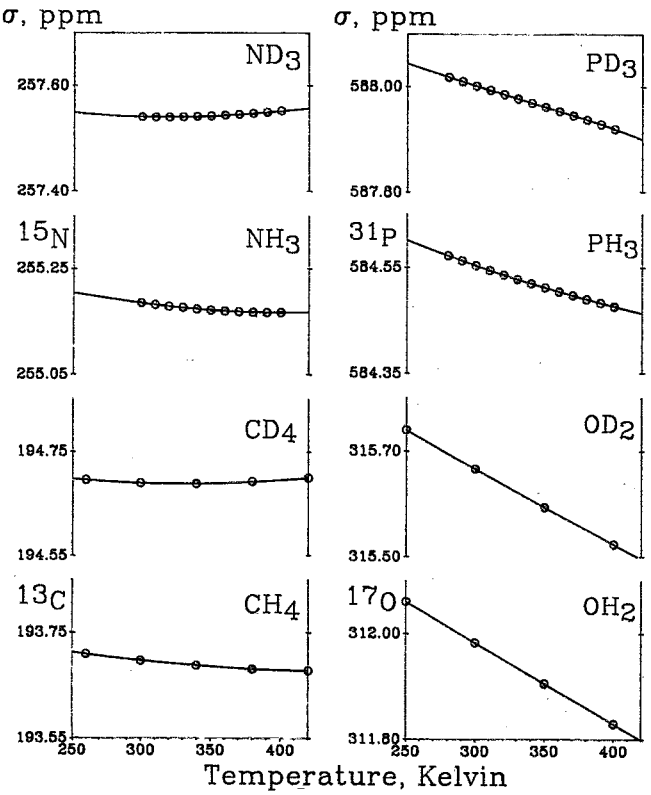


FIG. 9. The calculated temperature dependence of the shielding of the heavy nucleus in $CH_4$, $NH_3$, $H_2O$, and $PH_3$, and their corresponding fully deuterated isotopomers.

The thermal average bond angles in $NH_3$, $PH_3$, and $H_2O$ are all larger than the equilibrium bond angles and they are larger than the equilibrium bond angle in $ND_3$, $PD_3$, and $D_2O$, respectively. The results appear to be a consequence of the rotational and vibrational averaging in these nonrigid molecules. In these three molecules the combined first- and second-order contributions of the bending coordinate to the vibrationally averaged shielding is opposite to that of the bond stretches.

The overall temperature dependence of the shielding in these molecules have similar shapes, as seen in Fig. 9. The similarities of these curves indicate a reasonably consistent physical picture. It should be pointed out that the $CH_4$ and $H_2O$ results were obtained by common origin conventional CHF calculations whereas $NH_3$ and $PH_3$ were obtained using LORG.

## CONCLUSION

The deuterium-induced isotope shift for both molecules, ammonia and phosphine, is dominated by contributions coming from bond stretching. The first and second derivatives of the shielding with respect to stretching coordinates are negative and this seems to be true for most molecules, explaining the universality of the negative sign in isotope shift data. On the other hand, the temperature dependence is a combination of contributions from centrifugal stretching and bond angle distortions. In the case of $^{15}$N shielding in $NH_3$ and the $^{31}$P shielding in $PH_3$, the dependence of the shielding on the symmetry coordinates become nearly superposable when scaled by the ratio of $\langle 1/r^3 \rangle_{np}$ for the atoms in their ground states, with the exception of the inversion coordinate. Finally, the exceptional cases of $^{15}$N in $NH_3$ and $^{31}$P in $PH_3$ have been resolved.

A comparison of the full shielding surfaces of $^{13}$C in $CH_4$, $^{15}$N in $NH_3$, $^{17}$O in $H_2O$, and $^{31}$P in $PH_3$ shows some general similarities and provide some insight into the general shape of shielding surfaces in small molecules.

## ACKNOWLEDGMENT

This research has been supported by the National Science Foundation (Grant No. CHE-8901426).

[1] H. Batiz-Hernandez and R. A. Bernheim, Prog. NMR Spectrosc. **3**, 63 (1967).
[2] P. E. Hansen, Prog. NMR Spectrosc. **20**, 207 (1988).
[3] R. E. Wasylishen, J. O. Friedrich, S. Mooibroek, and J. B. Macdonald, J. Chem. Phys. **83**, 548 (1985).
[4] C. J. Jameson, J. Chem. Phys. **66**, 4983 (1977).
[5] D. B. Chesnut, Chem. Phys. **110**, 415 (1986).
[6] R. Ditchfield, Chem. Phys. **63**, 185 (1981).
[7] C. J. Jameson and H. J. Osten, Ann. Reports NMR Spectrosc. **17**, 1 (1986).
[8] C. J. Jameson, Bull. Magn. Reson. **3**, 3 (1980).
[9] C. J. Jameson, A. K. Jameson, and H. Parker, J. Chem. Phys. **68**, 2868 (1978).
[10] C. J. Jameson, A. K. Jameson, S. M. Cohen, H. Parker, D. Oppusunggu, P. M. Burrell, and S. Wille, J. Chem. Phys. **74**, 1608 (1981).
[11] C. J. Jameson, A. C. de Dios, and A. K. Jameson, J. Chem. Phys. **95**, 1069 (1991).
[12] C. J. Jameson, A. de Dios, and A. K. Jameson, Chem. Phys. Lett. **167**, 575 (1990).
[13] C. J. Jameson and H. J. Osten, J. Chem. Phys. **82**, 4595 (1985).
[14] A. D. Buckingham and J. A. Pople, Disc. Faraday Soc. **22**, 17 (1956).
[15] R. Ditchfield, Mol. Phys. **27**, 789 (1974).
[16] K. Wolinski, J. Hinton, and P. Pulay, J. Am. Chem. Soc. **112**, 8251 (1990).
[17] M. Schindler and W. Kutzelnigg, J. Chem. Phys. **76**, 1919 (1982).
[18] A. E. Hansen and T. D. Bouman, J. Chem. Phys. **82**, 5035 (1985).
[19] J. C. Facelli, D. M. Grant, T. D. Bouman, and A. E. Hansen, J. Comput. Chem. **11**, 32 (1990).
[20] RPAC version 8.5, Thomas D. Bouman, Southern Illinois University at Edwardsville, and Aage E. Hansen, H. C. Oersted Institute, Copenhagen, Denmark. GAUSSIAN88, M. J. Frisch, M. Head-Gordon, H. B. Schlegel, K. Raghavachari, J. S. Binkley, C. Gonzalez, D. J. Fox, R. A. Whiteside, R. Seeger, C. F. Melius, J. Baker, R. Martin, L. R. Kahn, J. J. P. Stewart, E. M. Fluder, S. Topial, and J. A. Pople, Gaussian, Inc., Pittsburgh, PA, 1988.
[21] D. A. Helms and W. Gordy, J. Mol. Spectrosc. **66**, 206 (1977).
[22] R. Krishnan, J. S. Binkley, R. Seeger, and J. A. Pople, J. Chem. Phys. **72**, 650 (1980).
[23] V. Spirko, J. M. R. Stone, and D. Papousek, J. Mol. Spectrosc. **60**, 159 (1976).
[24] P. W. Fowler, G. Riley, and W. T. Raynes, Mol. Phys. **42**, 1463 (1981).
[25] L. S. Bartell, J. Chem. Phys. **38**, 1827 (1963).
[26] M. Toyama, T. Oka, and Y. Morino, J. Mol. Spectrosc. **13**, 193 (1964).
[27] J. L. Duncan and D. C. McKean, J. Mol. Spectrosc. **107**, 301 (1984).
[28] C. J. Jameson and A. K. Jameson, J. Magn. Reson. **32**, 455 (1978).
[29] R. E. Wasylishen and J. O. Friedrich, Can. J. Chem. **65**, 2238 (1987).
[30] P. Lazzeretti and R. Zanasi, J. Chem. Phys. **72**, 6768 (1980).
[31] U. Fleischer, M. Schindler, and W. Kutzelnigg, J. Chem. Phys. **86**, 6337 (1987).

[32] D. B. Chesnut and C. K. Foley, J. Chem. Phys. **85**, 2814 (1986).
[33] T. D. Bouman and A. E. Hansen, Chem. Phys. Lett. **175**, 292 (1990).
[34] P. B. Davies, R. M. Neumann, S. C. Wofsy, and W. Klemperer, J. Chem. Phys. **55**, 3564 (1971).
[35] W. H. Flygare, J. Chem. Phys. **41**, 793 (1964).
[36] S. Rothenberg, R. H. Young, and H. F. Schaefer III, J. Am. Chem. Soc. **92**, 3243 (1970).
[37] T. D. Gierke and W. H. Flygare, J. Am. Chem. Soc. **94**, 7277 (1972).
[38] R. G. Barnes and W. V. Smith, Phys. Rev. **93**, 95 (1954).
[39] C. J. Jameson and A. D. Buckingham, J. Chem. Phys. **73**, 5684 (1980).
[40] C. J. Jameson and H. S. Gutowsky, J. Chem. Phys. **40**, 1714 (1964).
[41] *Multinuclear NMR*, edited by J. Mason (Plenum, New York, 1987).
[42] *NMR and the Periodic Table*, edited by R. K. Harris and B. E. Mann (Academic, New York, 1978).
[43] C. J. Jameson and H. J. Osten, J. Am. Chem. Soc. **107**, 4158 (1985).
[44] J. C. Duchamp, M. Pakulski, A. H. Cowley, and K. W. Zilm, J. Am. Chem. Soc. **112**, 6803 (1990).
[45] P. Lazzeretti, R. Zanasi, A. J. Sadlej, and W. T. Raynes, Mol. Phys. **62**, 605 (1987).
[46] S. G. Kukolich, J. Am. Chem. Soc. **97**, 5704 (1975).